

# Improvement of form accuracy and surface integrity of Si-HDPE hybrid micro-lens arrays in press molding



Ahmad Rosli Abdul Manaf<sup>a,b</sup>, Jiwang Yan<sup>a,\*</sup>

<sup>a</sup> Department of Mechanical Engineering, Keio University, Yokohama 223-8522, Japan

<sup>b</sup> Faculty of Manufacturing Engineering, Universiti Malaysia Pahang, 26600 Pekan, Pahang, Malaysia

## ARTICLE INFO

### Article history:

Received 24 May 2016

Received in revised form

12 September 2016

Accepted 30 September 2016

Available online 15 October 2016

### Keywords:

Hybrid optics

Lens array

Infrared lens

Press molding

Microstructure

## ABSTRACT

Press molding of silicon (Si)/high-density polyethylene (HDPE) composite is an important technology for producing thin hybrid infrared (IR) optics with microstructures. In this research, Si-HDPE hybrid micro-lens arrays were press molded under various conditions, and the form accuracy and surface integrity of the molded lenses were evaluated. Air trapping occurs inside the micro-lens cavities during molding in a non-vacuum environment, which leads to severe surface defects. To investigate the air trapping phenomenon, a new in-situ observation system was developed which enables real-time direct observation of the molding process. From the in-situ observations, it was found that air traps were formed among the HDPE pellets during melting, and an increase in the pressing force will increase the pressure of the trapped air, forming trenches on the lens surface. The trapped air also impacts the mold coating, causing trench formation on the coating surface. To minimize air trapping, the molding temperature, and pressing force must be strictly controlled. By performing press molding in a vacuum environment, trench formation was completely eliminated. Moreover, polymer shrinkage compensation was performed to improve the lens form accuracy.

© 2016 Elsevier Inc. All rights reserved.

## 1. Introduction

Press molding and hot embossing are effective processes for forming microstructures and high aspect ratio optical components of glass and polymers [1–5]. In most of the press molding and hot embossing processes, glass and polymer are heated above their glass transition temperature ( $T_g$ ), followed by the pressing stage. After the cooling stage with applied pressure, the part is removed and the microstructures are copied from the molds to the parts. In press molding, high precision microstructures can be formed under precisely controlled conditions, namely molding temperature and force, to improve the shape transferability, surface quality, and interface strength [6,7]. Using the press molding method, in our previous research, we successfully obtained Si-HDPE adhesion and formed a mechanical lock to form a hybrid IR lens substrate [8].

In press molding and hot embossing of microstructures, air trapping is a critical issue which highly impacts the surface integrity of the final part. The trapped air prevents the polymer from completely filling the cavities of the mold [9]. The trapped air has also been reported to form a pattern on the formed surface [10]. In press

molding of Si-HDPE hybrid lenses in a non-vacuum environment, we also confirmed the presence of air trapping induced surface defects on the pressed lenses, which creates the interface gap between the Si-HDPE substrates. However, the formation mechanism of the air trapping is not clear yet. Especially, in the present work, we used HDPE pellets instead of a polymer plate which has been used in hot embossing, but the impact of the use of polymer pellets as raw material on air trapping has not yet been investigated before.

Finite element simulation is used extensively to predict the behavior of the air trap during the molding process [11,12]. However, up to date, there is few experimental study on real-time direct observation of the air trapping phenomenon during press molding [13,14]. As of yet, the effects of trapped air on the performance of mold coating have not yet been clarified. In this study, we constructed an in-situ real-time observation system for clarifying the air trapping phenomenon during the press molding of the Si-HDPE hybrid lenses.

To solve the problem of air trapping, normally evacuation tools are required for the air to escape and are often used in micro-injection molding [1,15]. Micro-aspiration mold cavities are also useful for air trap ventilation [16]. However, it is not clear whether there are other methods to eliminate air trapping, such as by using

\* Corresponding author.

E-mail address: [yan@mech.keio.ac.jp](mailto:yan@mech.keio.ac.jp) (J. Yan).

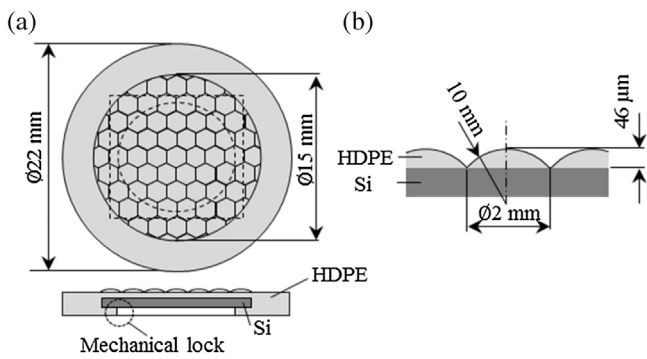


**Fig. 1.** Schematic diagram of: (a) Si-HDPE hybrid lens array design, and (b) lens cross section.

vacuum molding environment and/or by controlling molding conditions.

This paper presents experimental results of the fabrication of a Si-HDPE hybrid micro-lens array using press molding in non-vacuum and vacuum conditions with different press molding parameters and different mold designs. The influences of the HDPE pellets on the air trapping phenomenon were directly observed, and the resulting lens form accuracy and surface integrity were investigated. Furthermore, the coatings on the molds were also examined to investigate the influence of trapped air on the coating surfaces.

## 2. Experimental procedures

### 2.1. Sample materials

In the experiments, micro lenses were formed on a HDPE thin film which is adhered to a Si substrate to form a hybrid structure.

**Table 1**  
Si material properties.

Material properties	Value
Type	P
Doping element	Boron
Resistance ( $\Omega$ cm)	27
Refractive index	3.5
Thickness ( $\mu$ m)	755
Surface roughness (Ra) (nm)	3.5

**Table 2**  
HDPE material properties.

Material properties	Value
Density ( $\text{g}/\text{cm}^3$ )	0.955
Melting point ( $^{\circ}\text{C}$ )	133
Softening temperature ( $^{\circ}\text{C}$ )	125
Shape	Pellets
Pellet size (mm)	Diameter 3 Height 3.5
Melt flow rate (at $190^{\circ}\text{C}$ , 21.2 N) ( $\text{g}/10$ min)	9
Refractive index	1.5

HDPE is a silane cross-linkable resin, where silane is capable of generating crosslinks and forming a chemical link network between non-polar surfaces [17,18]. Cylindrical HDPE (LINKLON HM600A) pellets, 3 mm in diameter, 3.5 mm in height, supplied by Mitsubishi Chemical Corporation, Japan were used. A boron-doped Si (*p*-type) wafer provided by Global Wafers Japan Co. Ltd. was used as the base for the HDPE lenses. The Si wafer measured  $755 \mu\text{m}$  in thickness and was two-sided polished. The wafer was cut into 15 mm squares as test pieces. The material properties of Si and HDPE can be found in Tables 1 and 2.

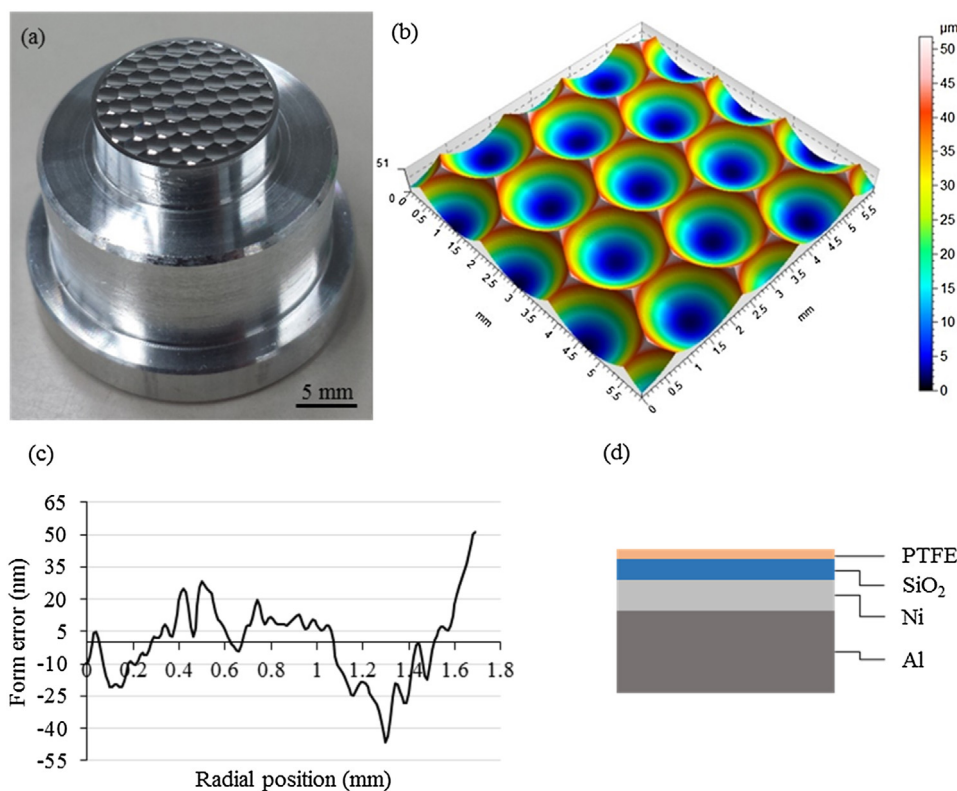


**Fig. 2.** (a) Photograph of an aluminum mold insert with micro-lens array, (b) three-dimensional topography of the mold, (c) form error profile of a micro-lens dimple on the mold insert, (d) layer structure of the mold insert coating.

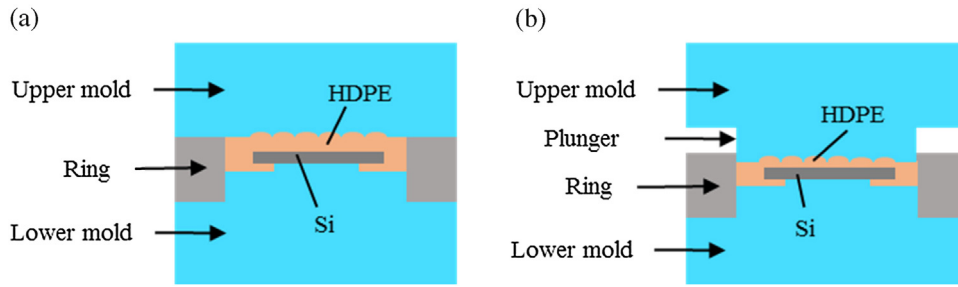


Fig. 3. Schematic diagram of molds (a) without a plunger, and (b) with a plunger.

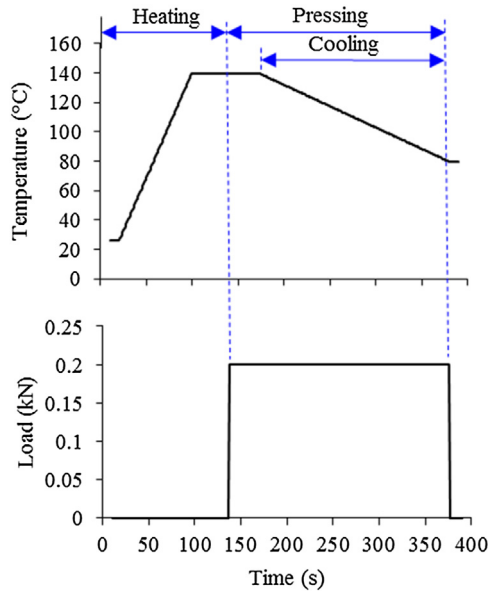


Fig. 4. Process parameters for hybrid lens press molding.

2.2. Hybrid lens structure

A plano-convex micro lens array with a Si-HDPE hybrid structure was designed as shown schematically in Fig. 1. The lens curvature radius was 10 mm, the diameter 2 mm, and the sag height 46 μm. The total diameter of the lens area was 22 mm, and the formed area of the lens was 15 mm in diameter. As per our previous research, a mechanical lock was used to surround the Si edges to improve strength of the hybrid structure.

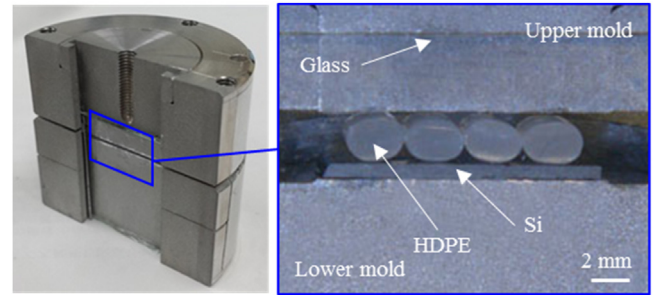


Fig. 5. Photograph of a cross-section of sliced molds.

2.3. Mold fabrication

The micro-lens array shapes were machined on an aluminum (Al) mold insert using an ultraprecision diamond lathe, NanoForm X (Ametech Inc., USA), which is equipped with an air bearing spindle. A single crystalline diamond tool with a nose radius of 250 μm was selected for the micro-cutting process. A constant spindle speed of 2700 rpm was used to roughly cut the surface with an 18 mm/min feed rate and a rough cut depth of 20 μm. The spindle speed was unchanged for the finishing cut, but the depth of cut was reduced to 4 μm while the feed rate was slowed down to 3.6 mm/min. A photograph of the mold insert and its three-dimensional topography are shown in Fig. 2(a) and (b), respectively. Fig. 2(c) shows a plot of form error distribution of a lens array, which was calculated by comparing the measured cross-sectional profile with the ideal lens profile. The peak-to-valley of form error was approximately 98 nm. Meanwhile, the surface roughness of the lens array of the mold was 3.3 nm Ra.

The lens array mold insert was coated with nickel (Ni), silicon dioxide (SiO<sub>2</sub>), and polytetrafluoroethylene (PTFE) to lower the surface adhesion energy during the demolding process. To improve the coating strength, Ni coating layer was first applied on the mold, fol-

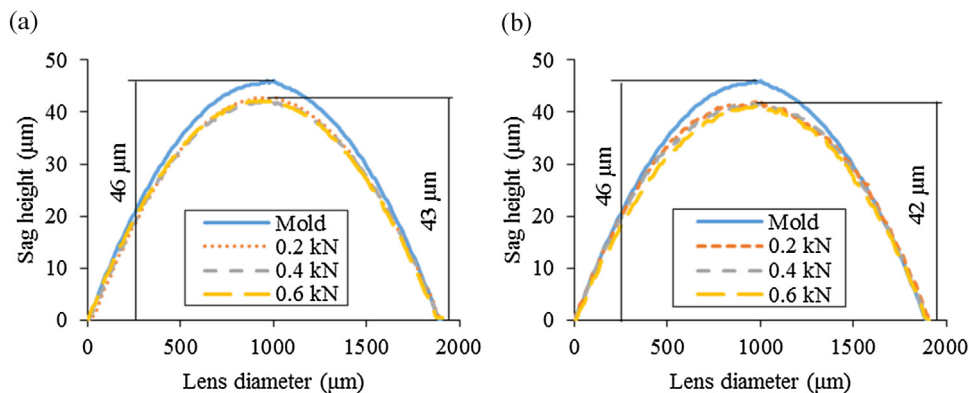


Fig. 6. Sag heights of lenses formed at different molding forces and different temperatures: (a) 133 °C, and (b) 140 °C, using the upper mold without a plunger.

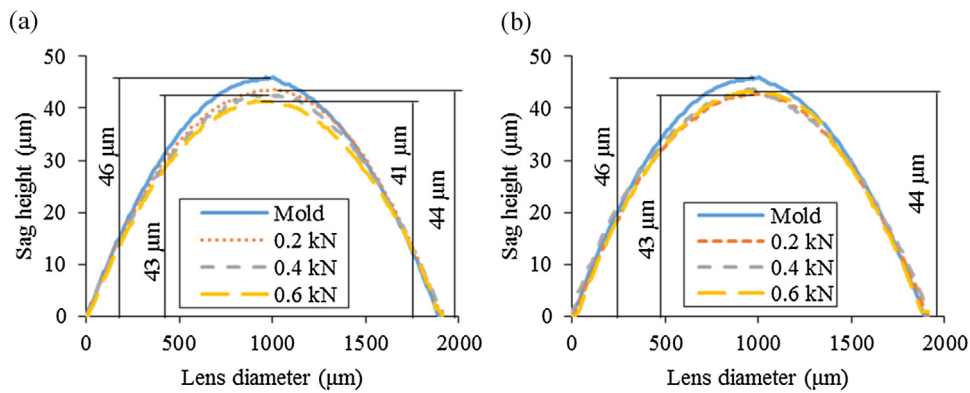


Fig. 7. Sag heights of lenses formed at different molding forces and different temperatures: (a) 133 °C, and (b) 140 °C, using the upper mold with a plunger.

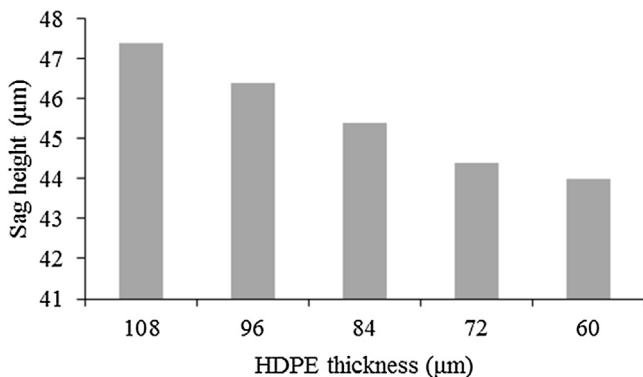


Fig. 8. Lens sag heights for different HDPE thicknesses.

lowed by SiO<sub>2</sub> layer [19]. The PTFE layer was then applied on SiO<sub>2</sub> layer, where bonding of both layers was reacted by oxygen (O) and hydroxide (OH). The coating layer were illustrated in Fig. 2(d). The thicknesses of the coatings were 20 nm, 10 nm, and one molecular layer, respectively, for the three coating materials. The PTFE coating provides lubrication on the mold surfaces to ease the part removal process [20]. Demolding is very important when removing a lens from the mold. Excessive demolding force can cause damage to the microstructures, which are caused by the sticking force between the mold and the polymer [21]. The coating process was performed by physical vapor deposition (PVD) in Geomatec Co. Ltd., Japan.

As illustrated in Fig. 3, the upper mold was comprised of two different designs. The first design was without a plunger while the second design was with a plunger. The effectiveness of the different upper mold design will be compared in the experiments. The other

side is the lower mold with an outer ring which functions as a mold cavity and holds the HDPE polymer during the molding process.

#### 2.4. Molding conditions

A glass molding machine GMP211 (Toshiba Machine Co. Ltd., Japan) was used for the fabrication of the Si-HDPE hybrid lenses. The machine is not equipped with a vacuum system. Instead, it is equipped with a transparent silica glass tube chamber which holds the purging nitrogen gas during molding to prevent oxidation of the mold at high temperatures. The molding temperature can rise up to 800 °C with a  $\pm 1$  °C tolerance and monitored by a thermocouple. The pressing force of the machine ranges from 0.2 kN to the maximum of 20 kN with a 0.98 N resolution. The lower mold movement accuracy towards the stationary upper mold is controlled by an AC servomotor with a resolution of 0.1  $\mu$ m.

In the experiments, two different melting temperatures were used, 133 and 140 °C. A temperature higher than 140 °C is not suitable as it will degrade the polymer and affect the IR properties [8]. The pressing forces used were 0.2, 0.4, and 0.6 kN. The sag height of the lens for different molding conditions will be compared to determine the best molding process parameters. The surface of the lenses and coating were also examined.

In this study, the isothermal molding method was used, where both the mold and molded materials are heated to the same temperature [22]. The molding process is schematically shown in Fig. 4, and the experimental steps are described as follows:

- 1) A Si substrate and a measured volume of HDPE pellets are placed into the mold cavity. The molding chamber is then closed.
- 2) The lower mold is raised closer to the stationary upper mold. A 2 mm gap is set between the two molds to enhance the heating

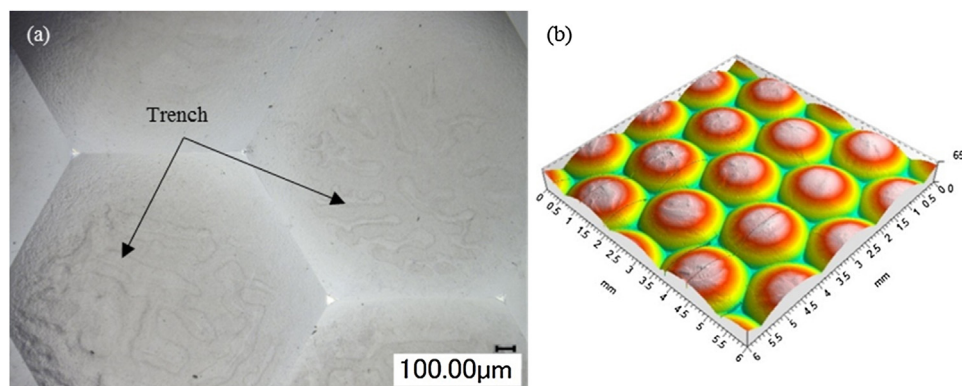


Fig. 9. (a) Photograph of trench formation on a lens surface and (b) three-dimensional topography of a Si-HDPE hybrid lens, showing an uneven lens surface.

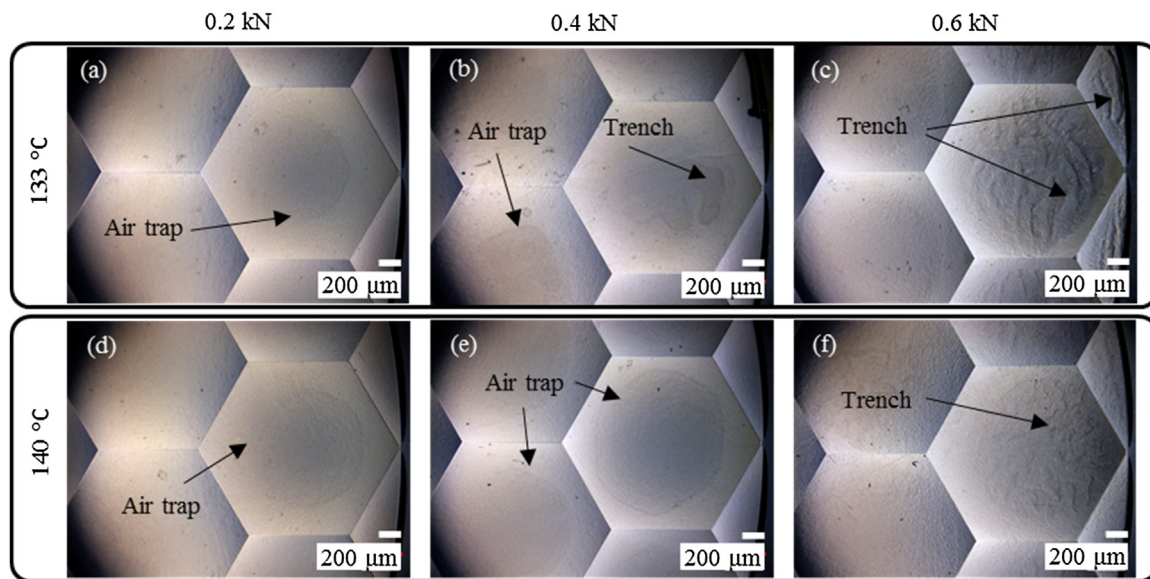


Fig. 10. Air trap and trench formation under different pressing forces and temperatures.

process. To prevent mold oxidation during heating, the chamber is purged with nitrogen gas for 20 s.

- 3) Both the molds and the specimen are heated with an IR lamp from room temperature to the molding temperature (133 or 140 °C) at a heating rate of approximately 0.6 °C/s.
- 4) The temperature is then maintained for 70 s, followed by the press molding until the mold is completely closed. The pressing force is set to 0.2, 0.4, and 0.6 kN.
- 5) The pressing force is maintained while nitrogen gas is introduced into the chamber again for cooling at a rate of approximately 0.3 °C/s until the mold temperature was 80 °C. The pressing force is maintained during cooling to prevent shear deformation at the substrate interface, which affects the adhesion strength while compensating for the shrinkage of HDPE.
- 6) Finally, the mold is opened and the molded Si-HDPE hybrid micro-lens is demolded from the molds and naturally cooled to room temperature. The time taken for a complete cycle of the press molding process was approximately 370 s.

### 2.5. In-situ air trapping observation

To investigate the air trapping phenomenon during the pressing process, we designed and fabricated a mold with a cross-sectional slice to observe how the HDPE pellets flow during pressing. As shown in Fig. 5, the mold was cut in half and included a slot feature. A glass plate was then attached into the slot, and a digital camera was used to record the flow of the polymer during the pressing process through the glass plate. To begin the in-situ observation, both the mold and the specimen were heated inside the quartz chamber to the required temperature. Once the temperature was reached, the chamber was opened immediately, enabling the pressing step to be captured.

### 2.6. Surface measurement and characterization

The lens topography measurements were performed after the molding process using a non-contact measuring machine, NH-

3SP (Mitaka Kohki Co, Japan), to avoid contact damage to the lens surfaces. It was equipped with a laser probe (semiconductor laser, wavelength 635 nm) which can scan the lens surfaces three-dimensionally. The vertical resolution of the machine is 1 nm, while the laser beam diameter was approximately 1 μm to ensure the narrow edges of the lens surface can be precisely measured. During the lens surface measurement, a horizontal resolution of 10 μm was selected. The topography obtained was then analyzed using the Talymap software (Taylor Hobson Ltd.), where the micro lens cross-section was obtained.

## 3. Results and discussion

### 3.1. Lens form error

In this study, for simplicity, the form error of the molded lens was evaluated by measuring the lens sag height. The sag height of the lens molded at pressing temperatures of 133 and 140 °C and pressing forces of 0.2, 0.4, and 0.6 kN are shown in Fig. 6. In the experiments, the first upper mold design without plunger was used. It can be seen that the lens sag height depends on the pressing temperature. Fig. 6(a) shows that the average sag height is about 43 μm at the pressing temperature of 133 °C. At a temperature of 140 °C, the sag height of the lens decreases to 42 μm, as shown in Fig. 6(b). The sag height difference was caused by polymer shrinkage during the cooling stage. The higher the molding temperature is, the larger the shrinkage rate is during the cooling stage [23].

In Fig. 6, it was found that at both temperatures, the pressing force had no significant effect on the lens sag height. This is because when the molds are closed, the upper mold and the ring on the lower mold get into contact, thus preventing them from further movement during cooling to compensate the HDPE shrinkage. From this meaning, the mold without a plunger is unsuitable for improving the lens form accuracy.

The second design of the mold, which had a plunger, was then used for comparison. Fig. 7(a) shows the lens sag height formed at a temperature of 133 °C under different pressing forces. The sag height was measured at 44 μm with the pressing force of 0.2 kN.

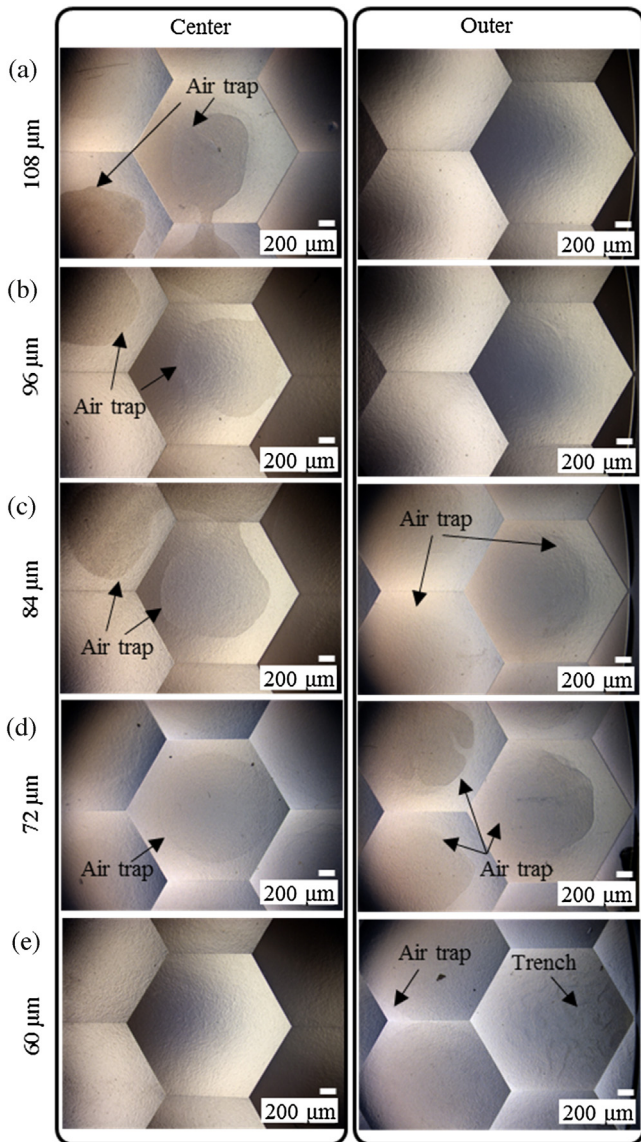


Fig. 11. Air trapping phenomena at different HDPE thicknesses.

The increase of pressing force to 0.4 and 0.6 kN has further reduced the sag height to 43 and 41  $\mu\text{m}$ , respectively. The reasons for sag height errors in Fig. 7(a) involve two aspects: air trapping at the apex of the lens during molding, and polymer shrinkage during cooling. The latter is not affected by pressing force, but the former is strongly affected by the pressing force. At a low temperature which causes a high polymer viscosity, a higher pressing force will cause a thicker air trap, as will be shown later in Section 3.3. As a result, the increase of the pressing force reduced the sag height. As shown in Fig. 7(b), the sag height was measured at 43  $\mu\text{m}$  when forming at a temperature of 140  $^{\circ}\text{C}$  with the pressing force of 0.2 kN. As the pressing force increased to 0.4 and 0.6 kN, the sag height accuracy was slightly increased to 44  $\mu\text{m}$ . At this temperature, the polymer viscosity is reduced, and the different pressing forces make a difference in the sag height. An increase in the temperature helps to decrease the viscosity of the polymer, thus improving the filling of the cavities [14]. The second design of the mold with a plunger is suitable because it can increase the cavity pressure during the pressing process. The plunger also provides additional movement during the cooling stage to compensate for polymer shrinkage.

Furthermore, the sag height of the lens also decreased with the reduction of the HDPE thickness on the Si substrate, as shown in

Fig. 8. The phenomenon might be due to the retarding flow of HDPE as the cavities become narrower [24].

### 3.2. Trench formation on lens surface

When the molding test was done in non-vacuum environment, sometimes trenches were formed on the lens surface, as shown in Fig. 9(a), leading to severe surface unevenness as shown in Fig. 9(b). The images of the lens surface which are formed at different molding temperatures and pressing forces are illustrated in Fig. 10. As a general trend, air trapping and trench occur in the center region at a low pressing force, and in the outer area of the lens array at high forces, as shown in Fig. 10(a)–(c). It might be due to that an increase of pressing force causes the movement of trapped air from the center of the lens array to the outside area of the lens during pressing. The results in Fig. 10 also indicate that the use of a small pressing force (0.2 kN) is better than a high pressing force (0.6 kN) to reduce the area of trapped air. In addition, as shown in Fig. 10(d)–(f), air trapping and trench formation are reduced when the lens is formed at a higher temperature (140  $^{\circ}\text{C}$ ). An increase in the temperature lowers the influence of molecular weight, and in turn, the viscosity of the polymer, thus suppressing the formation of trenches [24,25].

The air trapping phenomenon was further investigated by pressing HDPE into different thicknesses. The images of the center and outer areas of the lens array obtained at various HDPE thicknesses are illustrated in Fig. 11. As shown in Fig. 11(a) and (b), an air trap occurs at the center of the lens array when HDPE has pressed thicknesses of 108 and 96  $\mu\text{m}$ . When the HDPE is further pressed, the trapped air moves from the center to the outer lens arrays, as shown in Fig. 11(c) and (d). As the HDPE is pressed to 60  $\mu\text{m}$  thick, the trapped air moves entirely to the outer area of the lens array and tends to escape from the lens array area. The remaining air at the outer area receives the molding pressure, and trenches are created on the top of the lens surface, as shown in Fig. 11(e).

### 3.3. In-situ air trapping observation

To investigate the air trapping phenomenon during the press molding, in-situ observation was performed using the newly developed observation unit. The images of the in-situ observation at a temperature of 133  $^{\circ}\text{C}$  are illustrated in Fig. 12. As shown in Fig. 12(a), air pockets are formed at the boundaries between HDPE pellets and upper mold as well as between Si substrate and HDPE pellets. Also, weld lines are formed at the boundaries between the HDPE pellets. During pressing, the air pockets become smaller and are flattened, as shown in Fig. 12(b)–(e). As a result, trapped air channels are formed on the lens surface. However, when the pressing continues, the trapped air escapes and vanishes as shown in Fig. 12(f). Due to excessive pressing, an overflow of the HDPE is seen inside the gap between the glass plate and the mold.

The images of the in-situ observation at a temperature of 140  $^{\circ}\text{C}$  are illustrated in Fig. 13. Weld lines are seen among the pellets but less obvious than those in Fig. 12. This is due to the decrease of HDPE viscosity with the temperature rise. However, air pockets still exist among the pellets, as shown in Fig. 13(a). When the HDPE pellets are further pressed, the weld lines started to vanish, and the air pockets size is reduced, as shown in Fig. 13(b) and (c). Air pockets cannot be clearly seen in Fig. 13(d). Then, with further pressing, air pockets vanished completely along an overflow of HDPE, as shown in Fig. 13(e) and (f).

Based on the above observations, Fig. 14 shows the schematic diagram of the weld lines and air pocket formation. It is demonstrated that the HDPE pellets contribute to the air trapping phenomenon. Differing from plastic injection molding, where the pellets are heated and mixed inside a barrel before injected into the mold, in the present study the pellets need to be mixed during

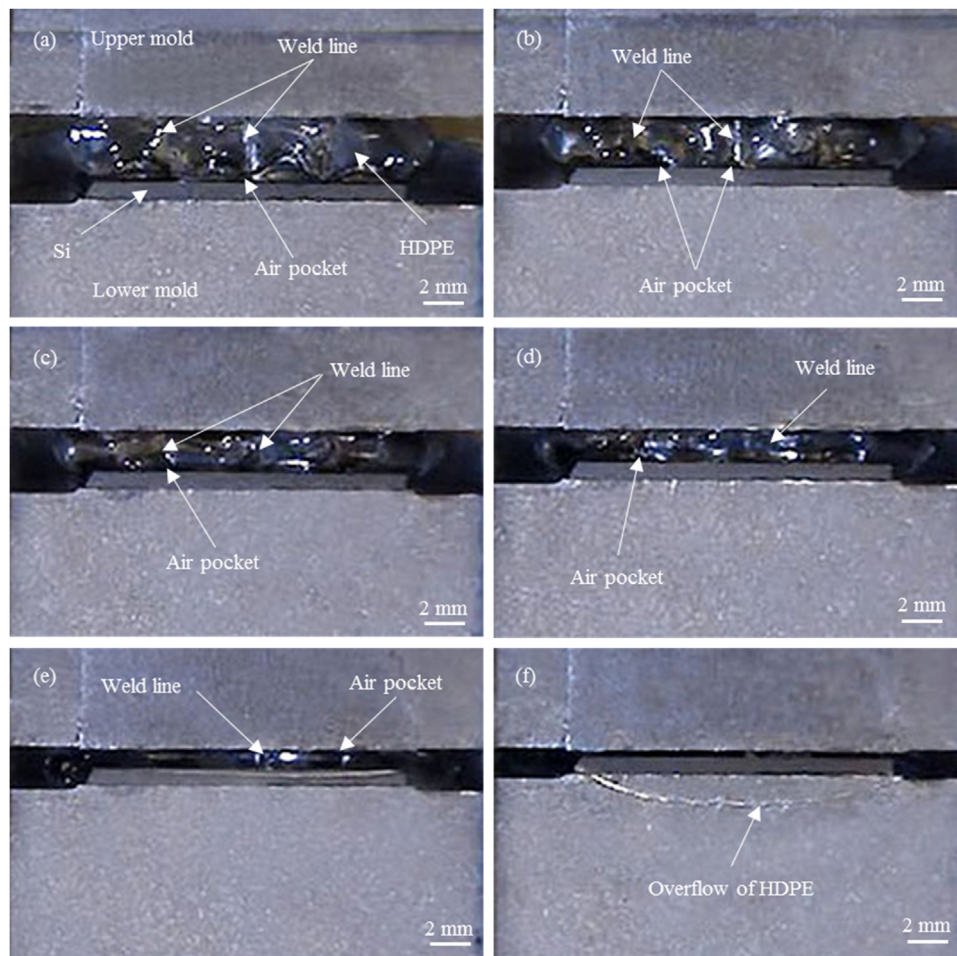


Fig. 12. In-situ air trapping observation results at 133 °C.

pressing. Weld lines and air pockets occur among the pellets which lead to air trapping.

To further clarify the effect of specimen shape on air trapping, instead of HDPE pellets, a flat HDPE plate with a diameter of 15 mm and a thickness of 1.5 mm was used for press molding at a temperature of 140 °C. The plate was made by melting and compressing HDPE pellets together before the molding experiments, because there were no HDPE plates commercially available. The in-situ observation result is shown in Fig. 15. In this case, no weld line and air pockets are found. Thus, from the meaning of preventing air trapping, a plate shape specimen is better than pellets. However, remelting the HDPE plate during press molding of lens arrays will cause deteriorations of the polymer properties [26].

#### 3.4. Trench formation on mold coatings

It has been known that mold coating will be worn out due to the alternating stress during a hot embossing and press molding process [27]. In this study, mold coating surface was examined after 80 cycles of press molding to investigate impact of trapped air on the coating. Fig. 16 shows scanning electron microscope (SEM) images of the mold coating surfaces. Trenches, which have similar patterns as those on the lens surfaces (see Fig. 9), are also formed on the mold coating surface. This fact indicates that the trenches formed on the lens surface due to the trapped air have affected the mold coating. The trapped air created non-uniformity of contact pressure distribution which consequently cause stress concentration in the

coating. The repetition of this kind of non-uniform contact cycles will peel off the coated layer, thus, trenches are created.

In addition to the trenches, the coating was also partially worn out, as illustrated in Fig. 16(c). HDPE adhesion to the mold coating was also confirmed, as shown in Fig. 16(d). Fig. 17(a) shows the error distribution profile of the mold after being used for 80 cycles. An average error of approximately 500 nm has been formed compared to the original mold profile, which is caused by trench formation, coating wear and HDPE adhesion.

The worn out phenomenon might have been caused by the HDPE polymer and the coating itself. The HDPE used in the experiments contained silane, which is used to achieve adhesion between HDPE and Si. However, there have been reports that silane can be used to strengthen the bonding of PTFE to its substrate [28]. Therefore, the silane-crosslinked HDPE may create an adhesion with the PTFE layer during molding. The repetition of contact and adhesion between the HDPE and the coating causes the wear of the coating, especially during demolding. Silane may also react with the SiO<sub>2</sub> layer after the peeling off of the PTFE layer, because the wear resistance of the PTFE itself is limited [29]. Fig. 17(b) shows the worn out phenomenon of PTFE/SiO<sub>2</sub> coatings. In some areas of the figure, the PTFE/SiO<sub>2</sub> layer has been removed, leaving the exposed Ni mold surface.

#### 3.5. Press molding in vacuum environment

In order to solve the air trapping problem, a press molding experiment was conducted in vacuum environment using a newly

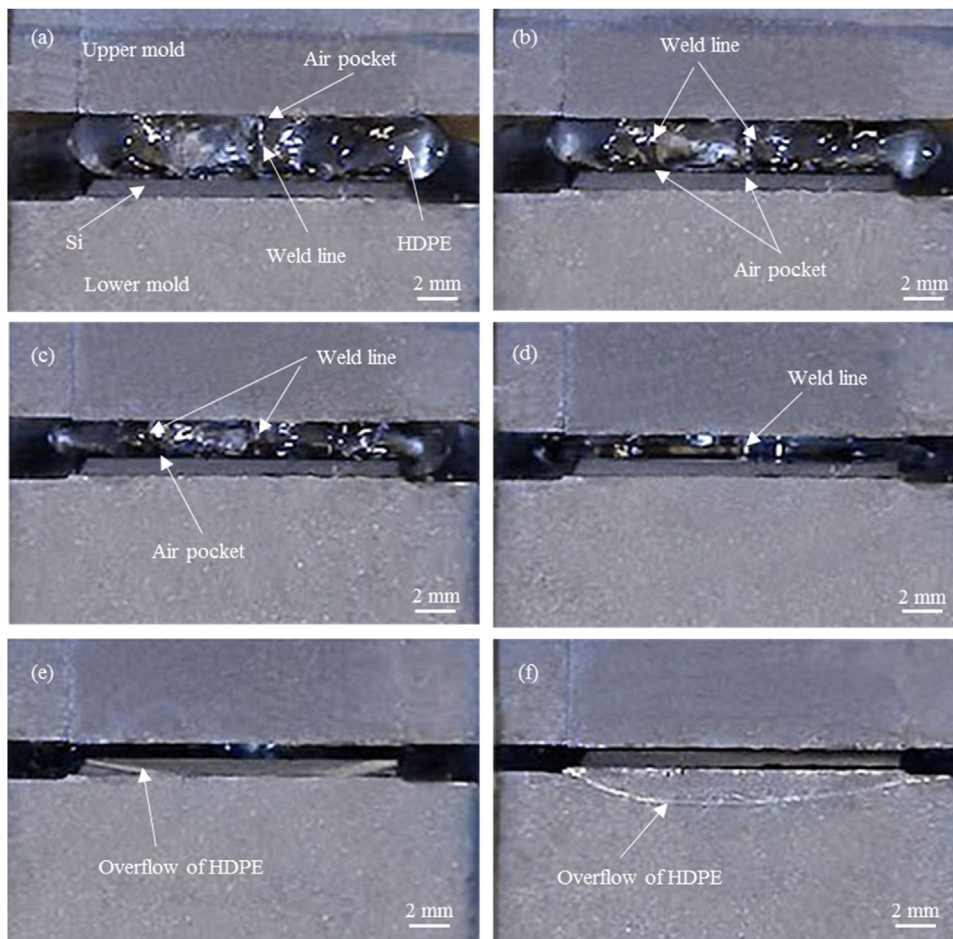


Fig. 13. In-situ air trapping observation results at 140 °C.

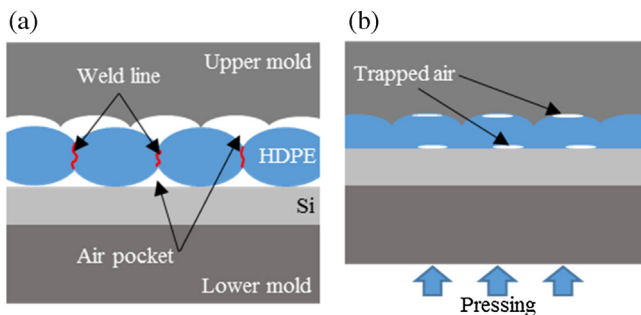


Fig. 14. Schematic diagram of (a) weld line and air pocket formation after heating, and (b) trapped air after pressing.

developed molding machine GMP-311V (Toshiba Machine Co. Ltd., Japan) that was equipped with a vacuum system. The pressing temperature was set to 140 °C while the pressing force was set to 0.2, 0.4, and 0.6 kN. The vacuum pressure was set to 0.1 Pa while the vacuuming time was 60 s. The rest of the press molding parameters were the same as per the previous experiment in a non-vacuum environment.

In the vacuum condition, since no air pockets are formed among the HDPE pellets during molding, no air trapping-induced surface defects were observed on the lens surface, as shown in Fig. 18. The press molded micro-lens array in Fig. 18(c) shows a perfect surface topography. These results indicate that the press molding in vacuum environment is crucial for achieving a high surface integrity without air trapping even using HDPE pellets as a raw material.

Finally, to further improve the form accuracy of the lens array by achieving the targeted lens sag height (46  $\mu\text{m}$ ), HDPE shrinkage compensation was included into the mold sag height during mold design, i.e., the sag height of the mold was designed to 49  $\mu\text{m}$ , 3  $\mu\text{m}$  bigger than the targeted lens sag height by considering the HDPE shrinkage rate. As shown in Fig. 19, the lens sag height was improved to 46  $\mu\text{m}$ , accurately the same as the targeted value. The use of different pressing forces 0.4, 0.6, and 0.6 kN had no significant effect on the lens sag height. Fig. 20 shows a photograph of pressed Si-HDPE hybrid lens arrays in the present study.

#### 4. Conclusions

Si-HDPE hybrid micro-lens arrays were formed by press molding under various conditions, and the form accuracy and the surface integrity of the fabricated lenses were evaluated. The following conclusions were obtained:

1. The mold with a plunger helps to improve the lens form accuracy. The plunger increases the cavity pressure and contributes to compensate for HDPE shrinkage during the cooling stage.
2. Air trapping and trench formation occur in the center region at a low pressing force, and in the outer area of the lens array at high forces. They are reduced when the pressing temperature increases.
3. By using the developed in-situ direct observation unit, the air trapping phenomenon during press molding was investigated. Air pockets were formed at the boundaries between the HDPE pellets and the Si substrate, and are flattened during the pressing



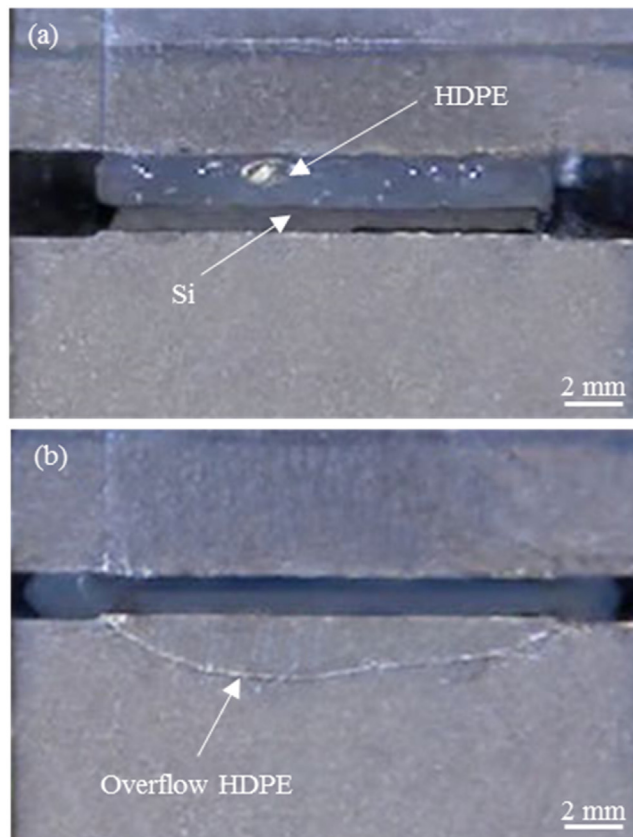


**Fig. 15.** In-situ air trapping observation for a flat shaped HDPE: (a) after heating, (b) after pressing.

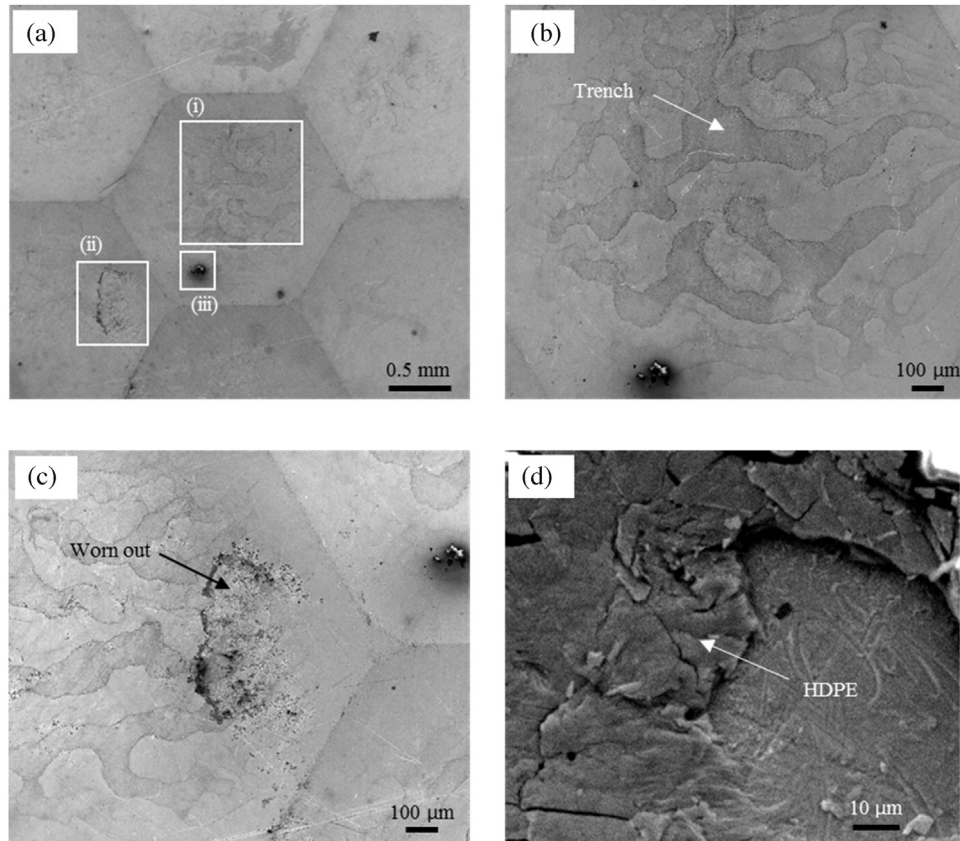


**Fig. 16.** (a) Surface of mold coating; (b) magnified view of rectangle (i) showing trench formation; (c) magnified view of rectangle (ii) showing worn out of coating; (d) magnified view of rectangle (iii) showing HDPE adhesion.

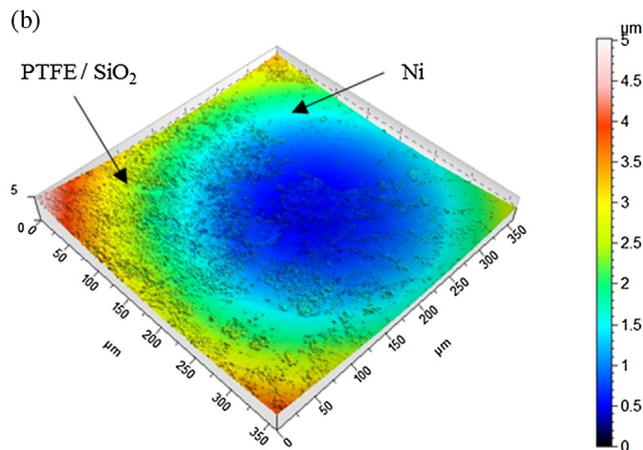
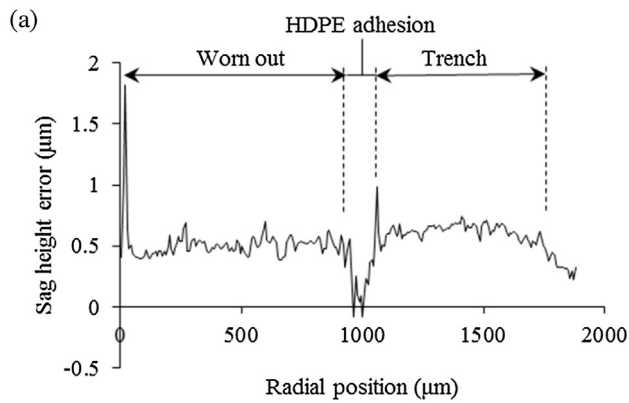


**Fig. 17.** (a) Cross-sectional profile of a micro-lens dimple on the mold, showing worn out, HDPE adhesion, and trench formation areas; (b) three-dimensional topography of mold surface showing worn out of coating.

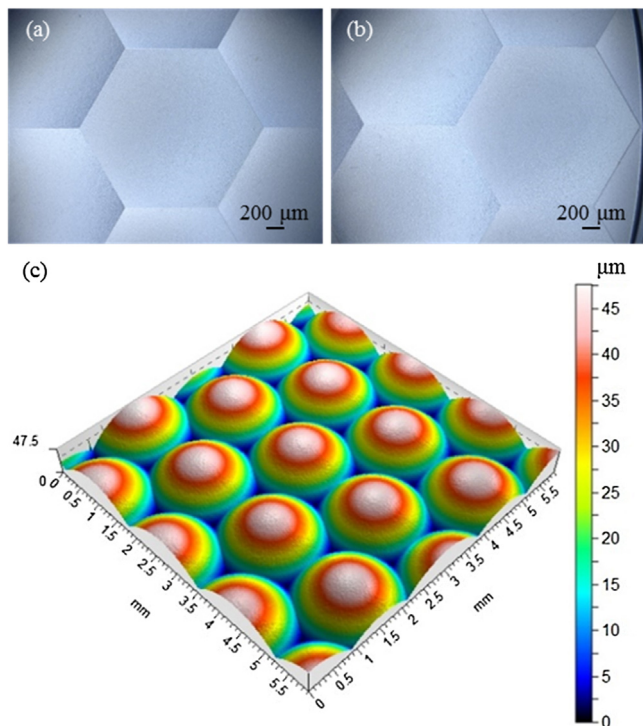


**Fig. 18.** A press molded Si-HDPE hybrid lens array in vacuum environment: (a) center region, (b) outer region, (c) three-dimensional topography.

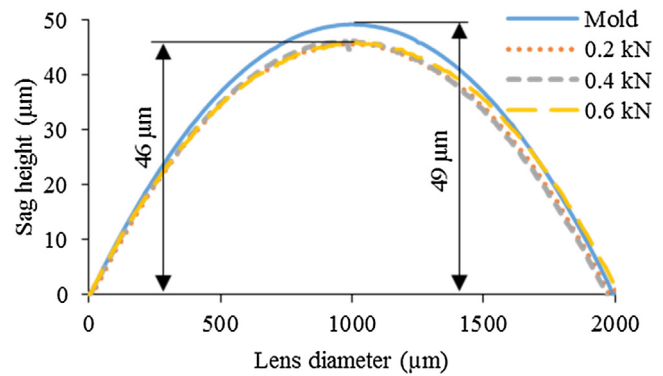


**Fig. 19.** Lens sag height obtained at different pressing forces in vacuum environment.

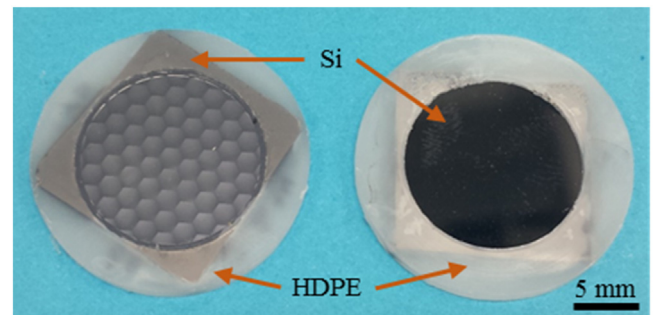


**Fig. 20.** Photograph of two pressed Si-HDPE lens arrays, showing different sides.

- process, forming trenches on the lens surface. Weld lines are formed at the boundaries among the HDPE pellets when pressing at 133 °C. Increasing the temperature to 140 °C minimizes the weld lines.
- Air trapping in molding press affects strongly the mold coating surface. Trench formation, wear marks and HDPE adhesion occur on the mold coating surface.
  - Molding a Si-HDPE micro-lens array in a vacuum environment helps to improve the lens surface integrity by completely eliminating air trapping and trench formation.
  - By compensating the HDPE shrinkage in mold shape design, the lens form accuracy is greatly improved.

#### Acknowledgements

The authors would like to thank Mitsubishi Chemical Corporation and Global Wafers Japan Co. Ltd, Japan for providing HDPE and Si samples and technical data. We also thank Toshiba Machine Co. Ltd, Shizuoka, Japan, for technical assistance in the pressing molding experiments using the GMP-311 V machine, and Dr. Tsunetoshi Sugiyama (Light for Wave Co., Japan) for his support during the lens design. This work has been partially supported by Keio University KLL Research Grant (000017) for Ph.D. Program for 2015 Academic Year, and Keio University Doctorate Student Grant-in-Aid Program 2015.

#### References

- Heckele M, Schomburg WK. Review on micro molding of thermoplastic polymers. *J Micromech Microeng* 2004;14:R1–14.
- Peng L, Deng Y, Yi P, Lai X. Micro hot embossing of thermoplastic polymers: a review. *J Micromech Microeng* 2014;24:013001.
- Kujawa I, Kasztelanic R, Stępień R, Klimczak M, Cimek J, Waddie AJ, Taghizadeh MR, Buczyński R. Optimization of hot embossing method for development of soft glass microcomponents for infrared optics. *Opt Laser Technol* 2014;55:11–7.

- [4] Hecke M, Bacher W, Müller KD. Hot embossing – the molding technique for plastic microstructures. *Microsyst Technol* 1998;4:122–4.
- [5] Yan J, Zhou T, Masuda J, Kuriyagawa T. Modeling high-temperature glass molding process by coupling heat transfer and viscous deformation analysis. *Precis Eng* 2009;33:150–9.
- [6] Yan J, Zhou T, Yoshihara N, Kuriyagawa T. KT: Shape transferability and microscopic deformation of molding dies in aspherical glass lens molding press. *J Manuf Technol Res* 2009;1:85–102.
- [7] Zhou T, Yan J, Masuda J, Oowada T, Kuriyagawa T. Investigation on shape transferability in ultraprecision glass molding press for microgrooves. *Precis Eng* 2011;35:214–20.
- [8] Abdul Manaf AR, Yan J. Press molding of a Si–HDPE hybrid lens substrate and evaluation of its infrared optical properties. *Precis Eng* 2016;43:429–38.
- [9] Taylor H, Lam YC, Boning D. An investigation of the detrimental impact of trapped air in thermoplastic micro-embossing. *J Micromech Microeng* 2010;20:065014.
- [10] Schiff H, Heyderman L, Auf der Maur M, Gobrecht J. Pattern formation in hot embossing of thin polymer films. *Nanotechnology* 2001:173.
- [11] Reddy S, Schunk PR, Bonnecaze RT. Dynamics of low capillary number interfaces moving through sharp features. *Phys Fluids* 2005;17:1–6.
- [12] Morihara D, Hiroshima H, Hirai Y. Numerical study on bubble trapping in UV-nanoimprint lithography. *Microelectron Eng* 2009;86:684–7.
- [13] Hocheng H, Nien CC. In-situ monitoring of cavity filling in nanoimprints by capacitance. *Japanese J Appl Physics, Part 1* 2006;45:5590–6.
- [14] Li JM, Liu C, Peng J. Effect of hot embossing process parameters on polymer flow and microchannel accuracy produced without vacuum. *J Mater Process Technol* 2008;207:163–71.
- [15] Giboz J, Copponnex T, Mélé P. Microinjection molding of thermoplastic polymers: a review. *J Micromech Microeng* 2007;17:R96–109.
- [16] Le Berre M, Shi J, Crozatier C, Velve Casquillas G, Chen Y. Micro-aspiration assisted lithography. *Microelectron Eng* 2007;84:864–7.
- [17] Xie Y, Hill CAS, Xiao Z, Militz H, Mai C. Silane coupling agents used for natural fiber/polymer composites: a review. *Compos Part A Appl Sci Manuf* 2010;41:806–19.
- [18] Baldan A. Adhesion phenomena in bonded joints. *Int J Adhes Adhes* 2012;38:95–116.
- [19] Gutsev D, Antonov M, Hussainova I, Grigoriev AYa. Effect of SiO<sub>2</sub> and PTFE additives on dry sliding of NiP electroless coating. *Tribol Int* 2013;65:295–302.
- [20] Sudagar J, Lian J, Sha W. Electroless nickel, alloy, composite and nano coatings – a critical review. *J Alloys Compd* 2013;571:183–204.
- [21] Guo Y, Liu G, Zhu X, Tian Y. Analysis of the demolding forces during hot embossing. *Microsyst Technol* 2006;13:411–5.
- [22] He Y, Fu J-Z, Chen Z-C. Optimization of control parameters in micro hot embossing. *Microsyst Technol* 2007;14:325–9.
- [23] Zhu X, Simon TW, Cui T. Hot embossing at viscous state to enhance filling process for complex polymer structures. *Microsyst Technol* 2011;18:257–65.
- [24] Chaix N, Gourgon C, Landis S, Perret C, Fink M, Reuther F, Mecerreyes D. Influence of the molecular weight and imprint conditions on the formation of capillary bridges in nanoimprint lithography. *Nanotechnology* 2006;17:4082–7.
- [25] Zhang T, He Y, Fu J. Simulation research on stress of polymeric patterns during micro hot embossing. *Appl Mech Mater* 2011;80–81:339–45.
- [26] Miu EV, Fox AJ, Jubb SH, Wakabayashi K. Morphology and toughness enhancements in recycled high-density polyethylene (rHDPE) via solid-state shear pulverization (SSSP) and solid-state/melt extrusion (SSME). *J Appl Polym Sci* 2016;133, n/a–n/a.
- [27] Wang Y, Zhang Q, Kuang X, Ding Y, Chen F, Liu H. Research on hot embossing process of high fill factor microlens array. *Microsyst Technol* 2014;21:2109–14.
- [28] Chen Y-C, Lin H-C, Lee Y-D. The effects of phenyltrimethoxysilane coupling agents on the properties of PTFE/Silica composites. *J Polym Res* 2004;11:1–7.
- [29] Zafarani HR, Abdi M, Bahrololoom ME. Wear behavior of PTFE/Hydroxyapatite composite fabricated by hot-press sintering process. *Acta Metall Sin (English Lett)* 2014;27:347–51.